

Electrodeposition of Horseradish Peroxidase (HRP) Enzyme on Polythiophenes / Polypyrrole / Polyaniline (PT/ PPY/ PANI) Substrate for Biosensor Application

Siti Amira Othman^{1*} and Shahidan Radiman²

¹Faculty of Applied Sciences and Technology, Universiti Tun Hussein Onn Malaysia, Pagoh, Johor

²Faculty of Science and Technology, Universiti Kebangsaan Malaysia, Bangi, Selangor

*Corresponding author (e-mail: sitiamira@uthm.edu.my)

Electrodeposition on substrates or monolayers is problematic as there are several factors influencing the process such as growth rate, temperature, humidity, substrate surface cleanliness, solubility, agglomeration and stability of the materials. These factors do not only inhibit the electrodeposition process but also present challenges to researchers. PANI, PPY and PT are conducting polymers that show excellent chemical, thermal and oxidative stability due to their low hydrogen content and aromatic structure. HRP is frequently used in conjugates to detect the presence of a protein target. In this study, Langmuir Blodgett (LB) and the layer by layer (LBL) method were used. PANI, PPY and PT acted as the polymeric support that was deposited on indium tin oxide (ITO) glass; HRP was added later by electrodeposition. The layers were characterized using UV-Visible (UV-Vis) spectroscopy, Fourier Transform Infrared Spectroscopy (FTIR), Atomic Force Microscopy (AFM), Variable Pressure Scanning Electron Microscopy (VPSEM) and the Four-Point Probe method. The results displayed the interactions and increased conductivity of each layer of the polymer. In an experiment that spanned 30 days, HRP exhibited decreased resistance at 4 °C compared to 27 °C and 60 °C.

Keywords: Electrodeposition; enzyme; polymer conjugate; biosensor

Received: November 2022; Accepted: January 2023

Polyaniline (PANI) films can be formed by mixing solutions, electrochemical methods and coating techniques. Ram & Malhotra [1], in their study on PANI film formation using the Langmuir Blodgett (LB) method, reported that when the subphase temperature was increased from 9.2 °C to 40 °C, the surface pressure increased from 27.5 to 28.2 mN m⁻¹. Interestingly, at the same temperature and a pressure of 25 mN m⁻¹, no change in the molecular area was observed. Moreover, the intensities of various peaks in the FTIR spectrum were clearly reduced with the increase in the number of monolayers. The polyemeraldine base monolayer was thermally stable at 19.2 - 40.0 °C.

Skotheim [4] explained that conduction polymers are functional polymers that convert the single and double carbon bonds along a polymeric chain. Long polymer conjugate chains allow for control of reversible chemical reactions, electrochemistry and physical properties through a doping/undoping process. Saxena & Malhotra [5] reported that conduction polymers such as polypyrrole (PPY), polythiophene (PT) and PANI have been commonly used in molecular electronic equipment. Through chemical modification and a doping process, the transition from the insulating stage to the conduction stage of a polymer can be observed [36].

Riul et al. [6] reported that PANI could be dissolved by doping it with protonic acids such as camphor sulfonic acid and toluene sulfonic acid, through which the central ions influenced the polymer solubility in the solvent. Monolayer condensation was obtained with high destructive pressures above 30 mN m⁻¹ when acidic subphases were applied. The pressure-isothermal graphs obtained for subphases containing hydrochloric acid (HCl) or trifluoroacetic acid (TFA) are typically similar. Solvent effects such as that of m-cresol (added before the film formation) further assist in the formation of a monolayer by creating a shape that results in increasing film flexibility.

Alkyl bonds that replace the back chains of the polymer, either covalently or electrostatically, typically improve the monolayer stability and displacement. Watanabe et al. [2] explained that in LB films, such bonds (alkyl bonds) produce high conductivity and a high degree of non-isotropy due to the presence of alkyl and hydrophobic chains between the polymer conduction planes. In the processing of LB polyaniline, water-soluble solvents such as N-methyl-2-pyrrolidone (NMP) have reportedly been used as the processing solvent. The use of NMP leads to the solubility of the material in the subphase and the formation of micro-clots on the water surface.

The self-assembly driving force of a poly-electrolyte layer by layer (LBL) is related to the electrostatic interaction of different groups of charge. The exchange between the positively and negatively charged species is necessary to ensure the successful application of this technique. In addition, ionic forces, hydrophobic properties, and weak charge transfers also influence the adsorption of polymer coatings [3]. The attractions between different charges occurs not only between molecular edge chain groups but also between dipolar, dipole-dipoles, Van der Waals, molecules in solvents and polymer hydrocarbon chains [39].

Anderson & Parks [7] explained that electrical conductivity can only occur through electronic transfer of a proton or hydronium ion. At high concentrations, only a few water molecules are ionized, whereby additional protons jump out of the molecules through a process known as a chain reaction. At high humidity, water condenses to fill the mesopores if the radius is not too large. This is due to the effect of surface tension and temperature [8]. Water surface adsorption is often non-uniform. Hydrophobic surfaces promote the growth of clusters of water molecules at relatively low humidity compared to hydrophilic surfaces. Fubini et al. [9] reported that this phenomenon tended to form multilayers while clustering occurred at almost 50 % of OH sites on hydrophobic surfaces.

HRP isoenzymes refer to a class III family of peroxidase plants including peroxidase from bacteria and spores [10]. This classification is based on amino acid sequences and three-dimensional structures inherent in enzyme classes. The structures of HRP C and other peroxidase plants contain three α -helices that are located at the core of peroxidase. The entire structure in this region is stabilized through disulfide bonds from Cys177 to Cys209. Mohsina & Khalil [11] reported the stability or resistance of radical species produced by peroxidase plants via catalytic reactions in a comparison of the structure and function of different peroxidases.

The incorporation of enzymes into electro-polymeric films has produced diverse properties which can be controlled and used in various micro-transducer applications. In terms of the capability of PPY/HRP films in comparison with that of H₂O₂, the former does not produce a response at 1 mV/s. According to a previous study [35], the signal increased when the film was prepared at 5 or 10 mV/s, and decreased at 50 mV/s with a response that was three times less than that at 10 mV/s. Polypyrrole monomers should be stored at 5 °C, protected from light and air [37]. There were different operating parameters that influenced the response of a biosensor such as the monomer, electrolyte and HRP concentration, temperature and the scan rate effect on electropolymerization [38].

Pauliukaite et al. [12] reported that there was an approach using intermediate molecules to allow enzymes to be immobilized onto a conduction polymer

matrix, which enabled electronic transfer between enzymes and electrodes. However, the entry of external molecules such as intermediates often leads to leaching and other problems. Thus, several enzyme-free intermediates for biosensors have been produced [13]. Alternatively, conduction polymers have functional groups that can also be used for enzyme immobilization processes.

Kumaran et al. [14] in their study on the electro-active properties of HRP/PANI reported that in addition to transferring electrical current, the maximum activity of an enzyme had to be maintained throughout the biochemical reaction to achieve maximum catalytic effectiveness. Morphological studies have proved that the properties of the surface of a conduction polymer depend on the preparation method, and this is important for effective enzyme stabilization. The electroactive properties of PANI should be in the range of pH 1 to 3 [40].

An accurate and rapid analysis of H₂O₂ content, especially in clinical control, environmental protection and the food industry, is required to produce high-quality products. Moralesa et al. [15] reported that the use of HRP-based biosensors could measure the rate of H₂O₂ produced. The HRP biosensor works by controlling the redox reaction of oxidized H₂O₂ during an enzyme reaction. The optimal response of a sensor can be obtained if the active site of the enzyme is oriented toward the conduction surface of the polymer [41].

The objectives of this research were to investigate the interactions between PANI, PPY, PT and HRP, as well as the attributes of the electrodeposition layer of HRP/PT/PPY/PANI.

EXPERIMENTAL

Chemicals and Materials

PANI emeraldine base (Product No.: 476706), PPY (Product No.: 577030), PT (Product No.: 699799), HRP (Product No.: P2088), dry disodium hydrogen orthophosphate salt (Na₂HPO₄) (Product No. 30158), potassium dihydrogen phosphate salt (KH₂PO₄) (Product No.: 7778-77-0) and *p*-toluene sulfonic acid (PTSA) were purchased from Sigma Aldrich. Methanol (CH₃OH) was obtained from Merck. Hydrogen peroxide (H₂O₂) was purchased from R&M chemicals. Deionized water was used to prepare all samples (Purelab Prima Elga, 18.2 M Ω electrical resistance). The purchased Indium Tin Oxide (ITO) glass was colourless and consisted of 90 % In₂O₃ and 10 % SnO₂ by weight.

Preparation of PANI, PPY and PT

PANI, PPY and PT were dissolved in 0.1 M methanol. PANI was prepared using the LB method. PANI was injected into a trough that contained *p*-toluenesulfonic acid (PTSA) at pH 1. The transfer pressure in the

trough solution was kept constant at 12 mN m^{-1} . The monolayer formed was deposited on a piece of Indium Tin Oxide (ITO) glass ($1.5 \text{ cm} \times 1.0 \text{ cm}$). After that, the monolayer PANI was dipped into the PPY solution, followed by the PT solution using the layer by layer method (LBL). The deposited PANI monolayer was dipped into the PPY solution using a dipper probe at a speed of 10 mm s^{-1} for the LBL procedure. The layer was immersed in the PT solution after the PPY/PANI had dried.

Electrodeposition Method

The electrodeposition approach was then used to deposit 0.1 mM HRP onto the PANI/PPY/PT layers. Phosphate buffer was used as the reaction media. The current was 750 A at 15 V , and the procedure took 5 minutes to complete.

Characterization of PANI, PPY, PT and HRP

The monolayer of PANI/PPY/PT/HRP was characterized with AFM for surface roughness and conductivity, VPSEM for morphology, the Four-Point Probe method for resistivity, UV-Vis spectroscopy for optical absorption spectra and FTIR for chemical bond identification.

RESULTS AND DISCUSSION

Relationships Between PANI, PPY, PT and HRP

Before performing the electrodeposition process, we investigated the effect and relationship of each polymer (PANI, PPY, PT) to HRP. This was done to observe the reactions and effects that took place. Samples were prepared by following the previous preparation method through which PANI was formed using the Langmuir Blodgett (LB) technique. On the other hand, the PPY and PT layers were deposited using the LBL technique. Figures 1, 2 and 3 show the UV-Vis spectra of PANI, PPY and PT with HRP. A similarity between the three figures was observed in terms of the increase in absorption rate when HRP was applied to each polymer.

PANI, PPY and PT are a family of conduction polymers that have the ability to absorb electromagnetic radiation due to their valence electrons that can be excited to higher levels. Figure 1 shows the two peaks in the HRP/PANI curve at 330 nm and 720 nm . The peaks indicate the disturbance in the PANI back chains due to $\pi\text{-}\pi^*$ displacement in the benzoid segment, as well as polaron disturbance. Each nitrogen atom has a hydrogen atom attached to it and half of the nitrogen atom has a positive charge due to the addition of protons.

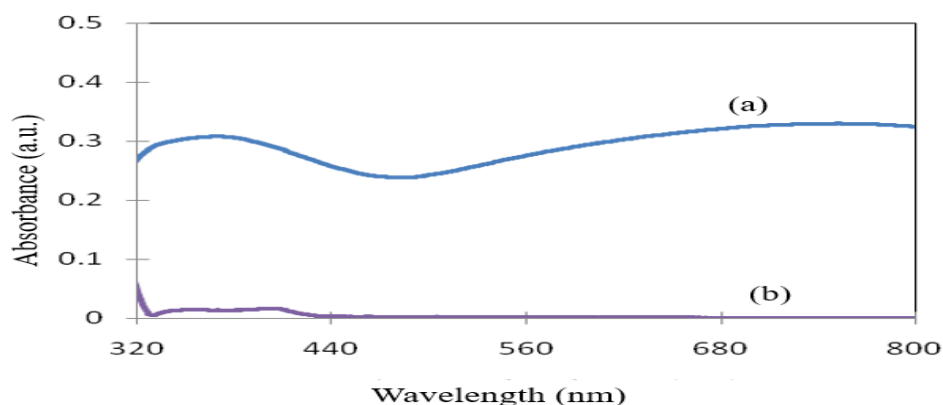


Figure 1. UV-Vis absorption spectra of (a) HRP/PANI (b) HRP

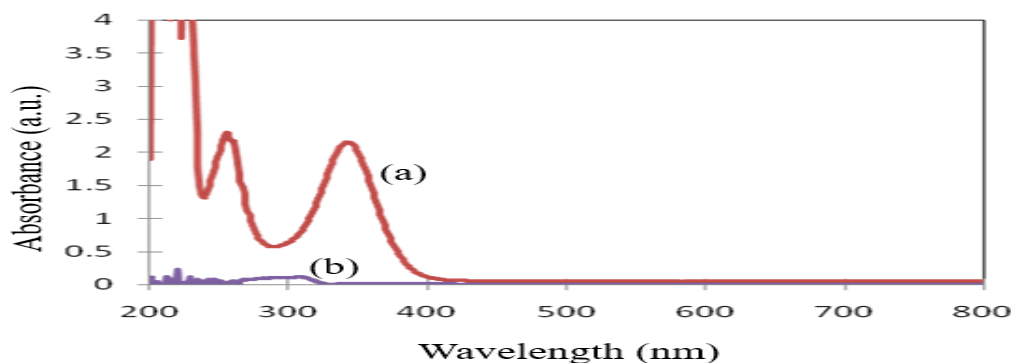


Figure 2. UV-Vis absorption spectra of (a) HRP/PPY (b) HRP

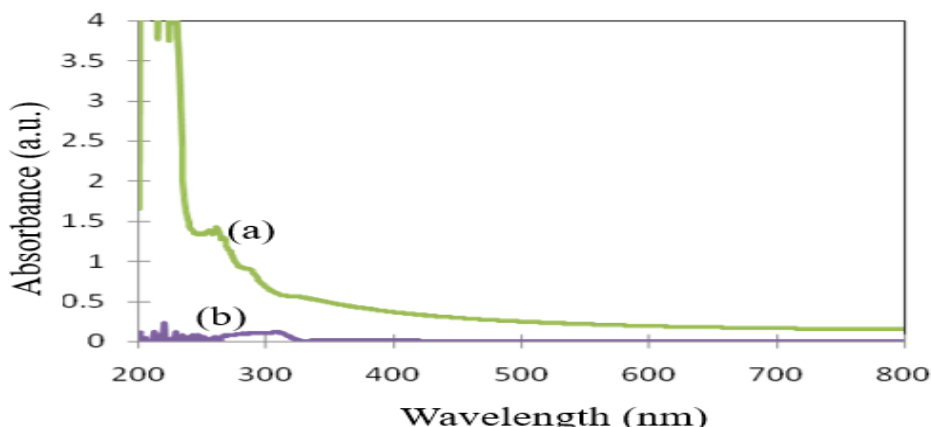


Figure 3. UV-Vis absorption spectra of (a) HRP/PT (b) HRP

The π - π^* transfer occurs when the nitrogen atoms in the second chain form a polaron [16]. This polaron forms a spiral gap and acts as a moving carrier charge in the system.

In Figure 2, there are three peaks at 210 nm, 280 nm and 350 nm. These three peaks are a result of the excitation of valence electrons to a higher level due to interference in the polymer chain [17]. An increase in the negative charge of the anion centre caused a reduction in absorption by PPY at a wavelength within the UV-Vis spectrum. Figure 3 illustrates the UV-Vis spectrum of HRP/PT, whereby the two peaks resulting from the reaction between the materials can be observed. These peaks at 210 nm and 280 nm signify the π - π^* transfer that occurred in the phenyl ring. The π dislocation reaction is responsible for producing the semiconductor properties of the material. The energy difference between the lower orbital (π) and the excited orbital (π^*) is known as the spiral gap [18]. The energy value of the spiral gap is determined via the electrical and optical properties of the semiconductor polymer. When the spiral gap energy is low, the π - π^* transfer becomes easy, thus producing high conductivity. The PANI spiral gap energy can be estimated from its UV spectra. Dislocation of electrons along the back chain of the conduction polymer, usually through π orbital overlap, causes charging to take place in the valence path [19].

Figures 1, 2 and 3 show that HRP produced peaks at 340 nm and 380 nm which correspond to the α -helix in the structure of HRP. The incorporation of HRP in all three polymers caused a disturbance at the nitrogen site on the polymer quinoid spiral. The HRP spectra in all figures depend on the interaction of HRP and the type of polymer. Peng Wang et al. [20] explained that HRP binds to polymers through a

crosslinking method, which shortens and condenses the polymer conjugate chains. This causes the absorption peak to shift to a shorter wavelength.

Figures 4 (a), (b) and (c) show the FTIR spectra of HRP/PANI, HRP/PPY and HRP/PT, which indicate the bonds between the polymers (PANI, PPY and PT) and HRP. In Figure 4 (a), there was a new peak at 3448 cm^{-1} which corresponds to the reaction between HRP/PANI. The peaks observed at 2450, 1070, 955, 864, 618 and 537 cm^{-1} are the result of stretching and vibrations in the chain $\text{N} = \text{quinoid} = \text{N}$. Whereas the peaks at 1263 and 518 cm^{-1} indicate the α -helix structure of HRP [21]. In Figure 4 (b), the peaks observed at 1264, 985, 864, 616, 518 cm^{-1} indicate the vibrations of the C - N bond in PPY. A shift in the peak at 2347 cm^{-1} to 2349 cm^{-1} corresponds to the doping process of PPY. There were also peak shifts at 1655 cm^{-1} and 2349 cm^{-1} due to the vibration of the -NH bond during the HRP/PPY reaction. The peaks indicating disturbances in the α -helix structure of HRP can be observed 517 cm^{-1} . Goel et al. [22] confirmed by FTIR the presence of additional bonds usually associated with a certain degree of crystallization. When the polymer chain is deposited, an additional vibration is triggered. In Figure 4 (c), the peaks observed at 2928, 1615, 1172, 1028, 906 and 695 cm^{-1} correspond to the C-S bond in PT. There was a peak shift from 2928 cm^{-1} to 2934 cm^{-1} indicating the doping stage of the PT. The peak observed at 1222 cm^{-1} signifies the α -helix structure in HRP (Nigel 2004). Analysis of the FTIR spectrum in Figure 4 (d) confirmed the existence of a new peak at 1201 cm^{-1} resulting from the immobilization of HRP on the PT/PPY/PANI layer [17]. In conclusion, Figures 4 (a) - (d) proved the presence of chemical bonds between HRP and PANI, PPY and PT, and the interrelationships between them.

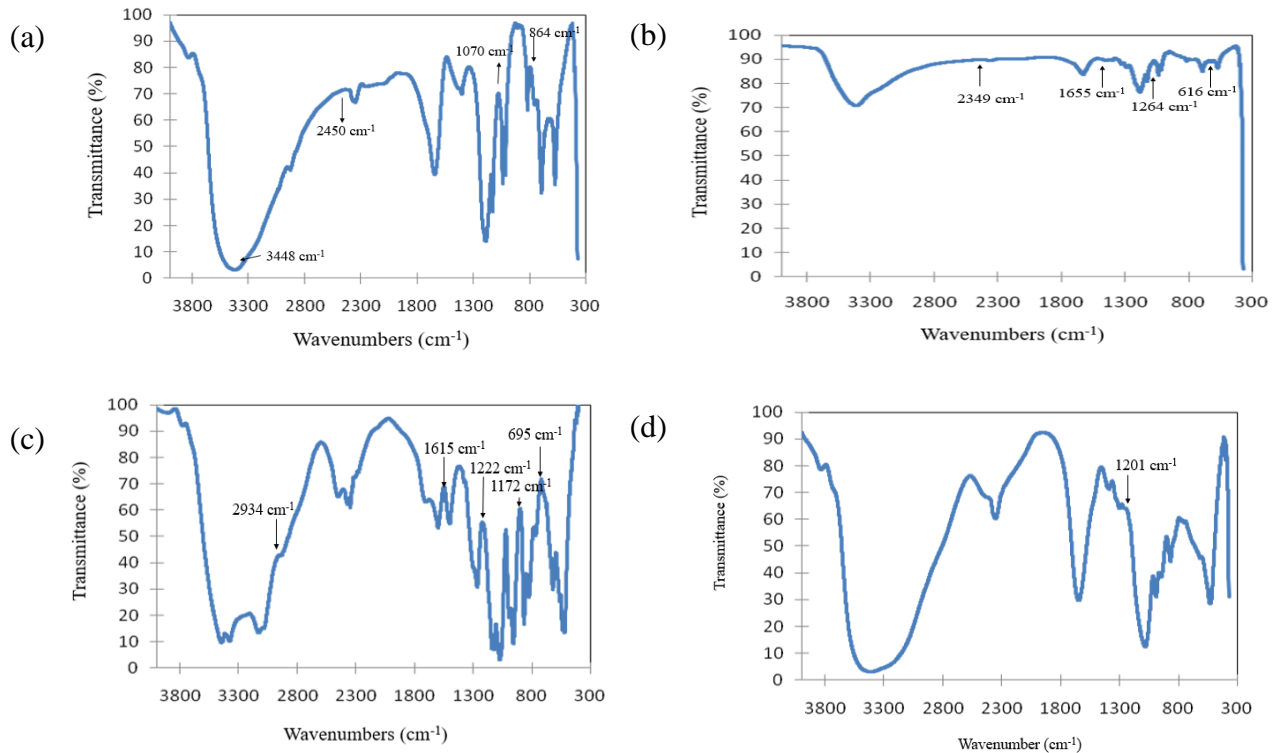


Figure 4. FTIR spectra of (a) HRP/PANI (b) HRP/PPY (c) HRP/PT (d) HRP/PT/PPY/PANI

Conductivity of PANI, PPY, PT, HRP and HRP/PT/PPY/PANI Layers

Figure 5 shows AFM images of (a) PANI, (b) PPY, (c) PT, (d) PT/PPY/PANI, and (e) HRP/PT/PPY/PANI that represent conductivity layers. Conductivity layers are coded in the same way as standard AFM images, whereby high conductivity regions are represented by brighter colours, while low conductivity regions are represented by darker colours [23]. The comparisons made between the images are based on the conductivity area. Conductivity is influenced by the molecular size of the polymer, the stage of deposition and the effect of the solution.

In these figures, PANI, PPY and PT exhibited bright yellow surfaces depicting their conductivity areas. The addition of PTSA as a doping material to the three polymers indirectly disrupted the polymer chain reaction and caused the excitation of their outer valence electrons to a higher level. Any changes in its chain can be explained by its optical absorption spectra (Figures 1, 2 and 3). The combination of the three polymers still provided conductivity although the addition of areas with dark colours can be observed. This is due to agglomeration that occurred as a result of the addition of polymer chains and the increase in surface density [24]. On the other hand, the deposition of HRP onto the surface of PT/PPY/PANI did not alter the conductivity regions of the polymer (Figure 5) as observed from the resistance values recorded for each layer as presented in Table 1.

The difference in the values recorded for film resistance between the polymers when HRP was immobilized onto the PT/PPY/PANI was not very large. This finding is supported by the AFM images presented in Figure 5, which show the conductivity region of the polymer, as well as when the HRP was immobilized onto the polymers. Table 1 shows that a reduction in resistance value caused an increase in the conductivity rate of the material. Omaish & Faiz [25] explained that the increase in conductivity could be attributed to three reasons: (1) an increase in carrier charge; (2) a decrease in the jump distance between conductive regions; and (3) an increase in conductivity area.

The three polymers used are conjugated polymers due to the presence of alternating single and double bonds on their polymer chains. This feature allows for the polymers to form decentralized electrons and provides spaces for reactions with other atoms. The dislocated electrons move along the system and act as charge carriers. The reaction with HRP causes the electrons to be removed from the back chain of the polymer, which produces cations. Electron addition also occurs, producing anions. Havriliak & Negami [26] reported that anions and cations act as charge carriers that jump from one place to another in the system under the influence of an electric field, which in turn increases the conductivity of the material. The conductivity of a polymer results from the oxidation and reduction processes that occur in the system, whereby the polymer may donate (oxidation) or

receive (reduction) electrons. When the polymer has been electronically charged, the opposite ions from the solution enter the polymer to produce a natural electrostatic charge. These ions are often referred to as doping materials. In conduction polymers, a carrier charge is generated in the polymer chain. The oxidation process breaks the double bonds of two polymers, which produces radicals and positive charges in the polymer chain known as

polarons [27]. The polarons form bipolarons at high concentrations, which then react with each other. The conductivity of the polymer is derived from the long chains of conjugates or double bonds that alternate in the polymer matrix. Electrochemical doping alters the overlapping forms of molecular orbitals and creates polarons or cation radicals that are free to move under the influence of electric fields.

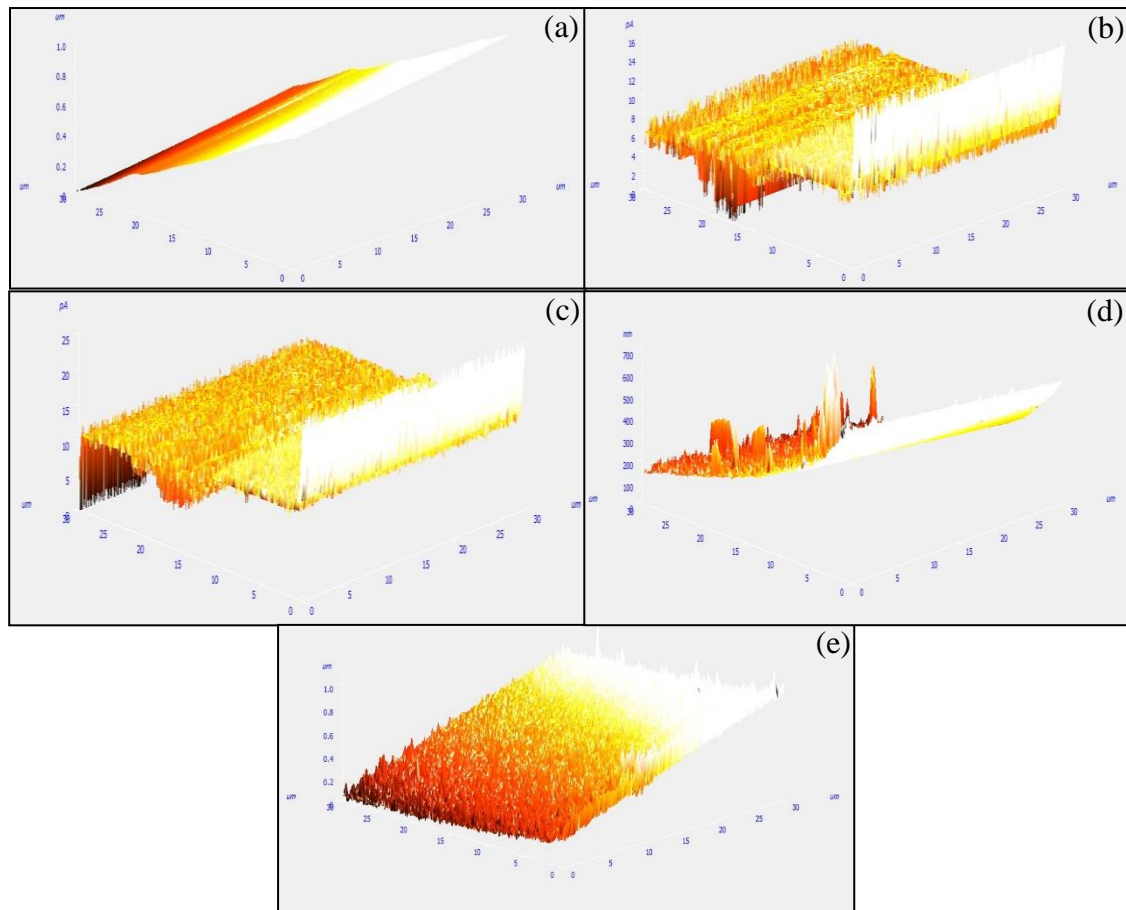


Figure 5. Conductivity surfaces of (a) PANI (μm), (b) PPY (ρA against μm), (c) PT (ρA against μm), (d) PT/PPY/PANI (μm) and (e) HRP/PT/PPY/PANI (μm)

Table 1. Comparison of sheet resistance value (ρ_s) for PANI, PPY dan PT film after HRP immobilization

Films	ρ_s (Ω^{-2})
PANI	$6.399 \times 10^7 \Omega^{-2}$
PPY	$7.000 \times 10^4 \Omega^{-2}$
PT	$8.000 \times 10^4 \Omega^{-2}$
PPY/PANI	$3.6256 \times 10^5 \Omega^{-2}$
PT/PPY/PANI	$2.7192 \times 10^5 \Omega^{-2}$
HRP/PANI	$6.174 \times 10^7 \Omega^{-2}$
HRP/PPY	$6.000 \times 10^4 \Omega^{-2}$
HRP/PT	$5.022 \times 10^4 \Omega^{-2}$
HRP/PT/PPY/PANI	$2.2660 \times 10^5 \Omega^{-2}$

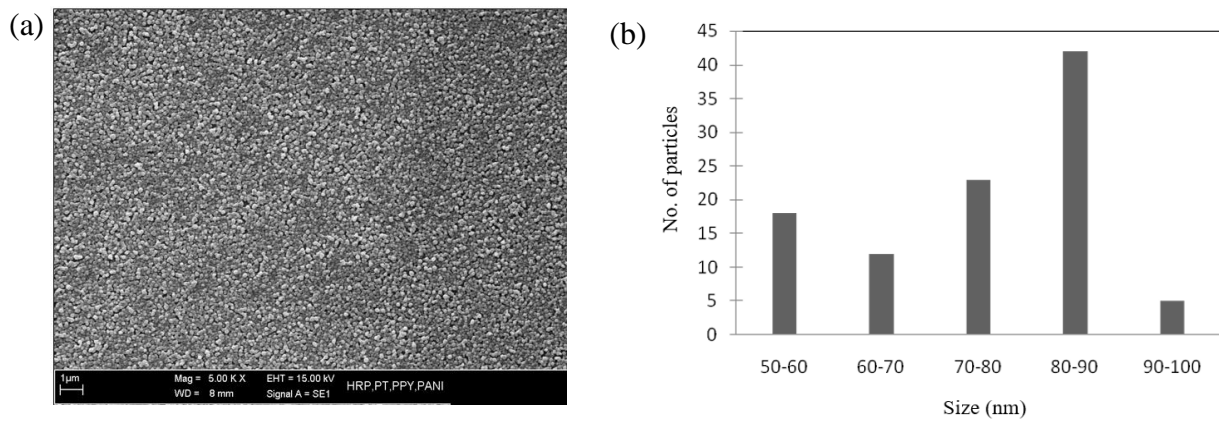


Figure 6. (a) VPSEM image of HRP/PT/PPY/PANI after electrodeposition; (b) Average particle size of HRP/PT/PPY/PANI

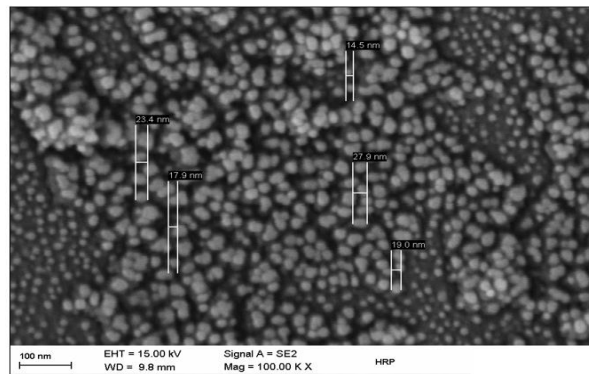


Figure 7. VPSEM image of HRP

Electrodeposition Layer of HRP/PT/PPY/PANI

The electrodeposition of HRP onto the PT/PPY/PANI layer produced a nearly uniform surface layer of HRP/PT/PPY/PANI with different particle sizes (Figure 6). Figure 6 (b) shows that most of the particles were in the range of 80–90 nm, due to the effect of the reaction between the surface layer and HRP. The empty pores formed in the PT/PPY/PANI layer further facilitated the immobilization process of HRP molecules. The small size of HRP (Figure 7) allows for easy absorption and adsorption onto the PT/PPY/PANI layer.

Kafi et al. [28] explained that an enzyme or protein usually has a large molecular mass and a flexible (deformed) structure. Such properties allow the molecule to react with any surface easily. Enzyme stabilization is important to maintain the activity and stability of the enzyme. Thus, the activity of an enzyme that is covalently bound to a particular molecule can become higher depending on the success of the stabilization process. Covalent bonding between biomolecules and polymer matrices can be formed through polymer synthesis or covalent immobilization.

Because immobilization occurs only at the outside of the polymer surface, optimal reaction conditions can be achieved at each step. Fernandes et al. [29] reported that enzyme immobilization was one of the most important steps in the fabrication of biosensors. The selection of the technique used to link the biological components (enzymes) to the transducer is important because the stability and lifespan of the biosensor depend on the shape of the enzyme layer. Furthermore, bioactive molecules such as enzymes, cells, etc., can be immobilized to form multilayers by controlling factors such as thickness, variable charge, enzyme activity and stability [30].

Figure 8 shows the AFM image of the PT/PPY/PANI before and after the deposition of HRP onto the polymer substrate by electroprecipitation. The deposition of HRP caused an increase in surface roughness due to its reactive nature. Thus the small-sized HRP (Figure 8 (b)) was able to enter the PT/PPY/PANI polymer pores. The FTIR spectrum in Figure 9 confirmed the formation of a new peak at 1201 cm^{-1} , which resulted from the reactive nature of the HRP that was adsorbed onto the PT/PPY/PANI layer [17].

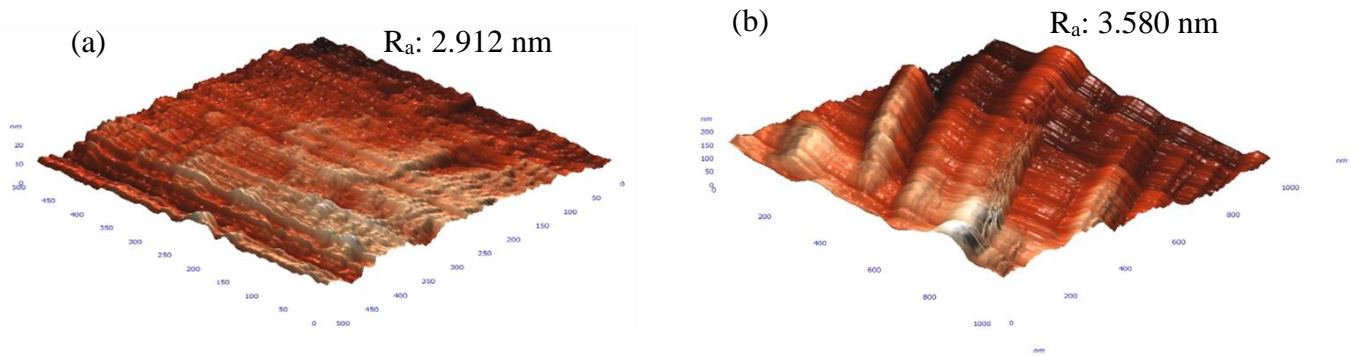


Figure 8. Difference between average roughness values (R_a) of (a) PT/PPY/PANI, and (b) HRP/ PT/PPY/PANI

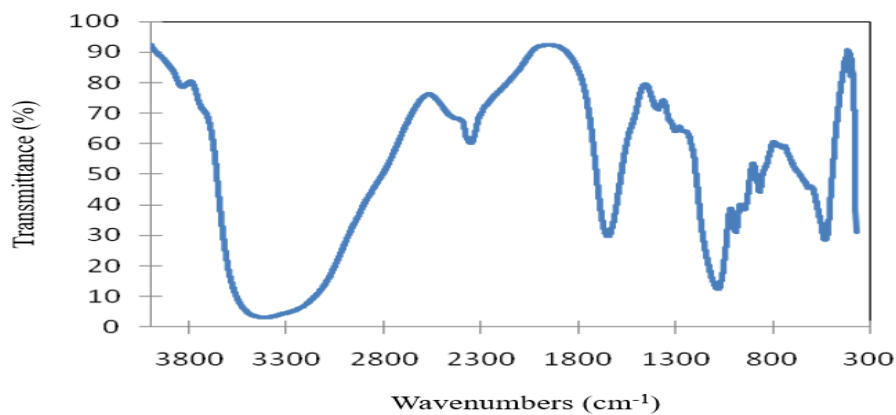


Figure 9. FTIR spectrum of HRP/PT/PPY/PANI

Effect of Temperature on the HRP/PT/PPY/PANI Layer

The HRP/PT/PPY/PANI electrode layers were observed at different temperatures (4 °C, 27 °C and 60 °C) for 30 days (Fig. 10). It was found that the resistance value became constant on day 21 at all tested temperatures.

At 4 °C, the resistance value began to decrease on day 25, demonstrating the suitability of the HRP/PT/PPY/PANI electrode layer for application under cold conditions. A study conducted by Chen et al. [31] suggested that the stability and activity of HRP could be achieved if the HRP electrode was placed in cool conditions.

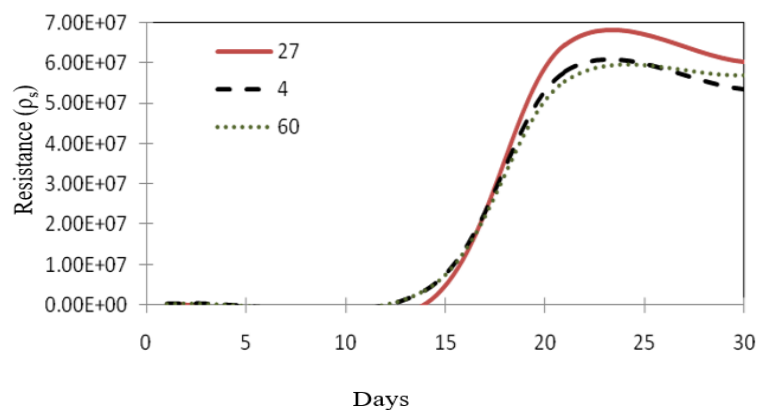


Figure 10. Film resistance of HRP/ PT/PPY/PANI at different temperatures: 4 °C, 27 °C dan 60 °C in 30 days.

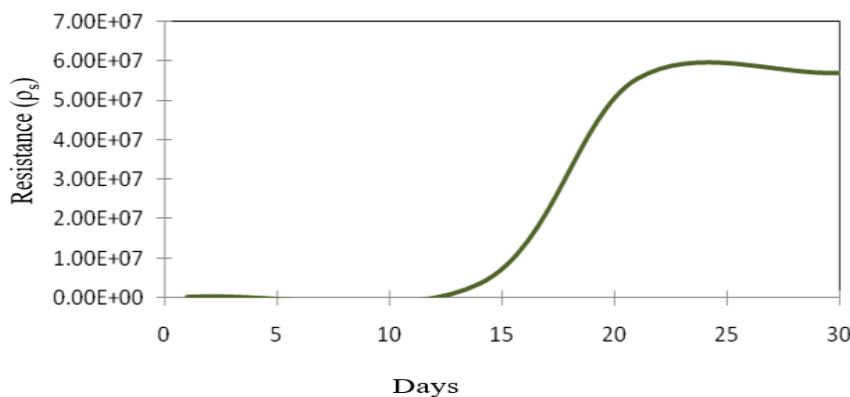


Figure 11. Film resistance of HRP/ PT/PPY/PANI in 30 days for $T=50\text{ }^{\circ}\text{C}$

Experiments were conducted at $4\text{ }^{\circ}\text{C}$ in this study due to the stability and high-level activity of HRP when placed in cool conditions [29], whereas $27\text{ }^{\circ}\text{C}$ was selected to observe the performance of the HRP/PT/PPY/PANI coating electrode at room temperature. Observation at $60\text{ }^{\circ}\text{C}$ was conducted to evaluate the effects of heat on the HRP/PT/PPY/PANI layer, as a previous study reported a decrease in conductivity at temperatures higher than $50\text{ }^{\circ}\text{C}$ [32]. The analysis was performed at these three different temperatures to evaluate the diversity and suitability of the electrodes for application in different conditions. At absolute zero, all stages in the valence path are filled with electrons, whereas all stages in the conduction path are empty, indicating no current flow. As the temperature increases ($60\text{ }^{\circ}\text{C}$), electrons are excited from the valence band into the conduction band through the band gap. Electrical conduction occurs through a small number of electrons in the conduction band [27]. A large number of electrons that remain in the valence band have limited movement because only a small number of voids exist, although the electrical conduction in the valence band causes the movement of a large number of electrons. This void, a hole, moves in the opposite direction to the electron and acts as an opposite charge carrier.

The HRP/PT/PPY/PANI electrodes can be used for up to 30 days by controlling external factors (e.g., temperature) that can affect the stability of the electrodes. Conductivity increased with an increase in temperature up to $50\text{ }^{\circ}\text{C}$ and then began to decrease at temperatures above $50\text{ }^{\circ}\text{C}$ (Fig. 11). The reduction in conductivity at temperatures over $50\text{ }^{\circ}\text{C}$ was due to electron rejection. As the temperature increased, the transfer of electrons from the valence gap to the conduction gap became easier and thus, increased the conductivity of the system [32]. However, temperatures higher than $50\text{ }^{\circ}\text{C}$ limit the localization of electrons from the valence gap to the conduction gap, causing repulsion among the nearby electrons and preventing them from reaching the conduction site. Therefore, above $50\text{ }^{\circ}\text{C}$, conductivity decreased with temperature. At $4\text{ }^{\circ}\text{C}$, the movement of molecules is minimal as they stay close to each other and the reaction between the molecules is weak or

non-existent. At $60\text{ }^{\circ}\text{C}$, the molecules move rapidly and electron excitation occurs due to the applied heat. The excitation further increases the conductivity of the material. On the other hand, at $27\text{ }^{\circ}\text{C}$, the intermolecular reaction is moderate and the rate of electron transfer in the system is less than that at $60\text{ }^{\circ}\text{C}$. In addition, conductivity increases with temperature due to the increased rapidity of the jumping and excitation of the charge carrier into the conduction loop [33]. As explained earlier, the conductivity decreased above $50\text{ }^{\circ}\text{C}$ due to limited electron dislocation. Although the movement of molecules was at a minimum at $4\text{ }^{\circ}\text{C}$, HRP was found to be stable and suitable for application under such conditions. This indirectly affects the rate of H_2O_2 detection. The HRP/PT/PPY/PANI coating electrodes were stored at $4\text{ }^{\circ}\text{C}$ when not in use.

Resistance Layer of HRP/PT/PPY/PANI

HRP is a type of enzyme that is capable of doubling weak voltages and improving signal reception [21]. Theoretically, this capability indirectly affects the resistance value of the HRP/PT/PPY/PANI layer. However, this study has found that there was no significant change observed in the resistance value, ρ_s of each layer (Table 1). Such an observation is due to the non-uniformity in the deposition layer, which exists as a result of agglomeration and reaction problems between molecules of different charges [19].

Impedance was used to measure the rate of electrical transfer in a system. Indirectly, it can measure the resistance rate and conductivity properties of the material. Current flows through the conductive material when a voltage is applied. The impedance measurement changes with the frequency of the applied voltage, and is related to the characteristics of the material. The shape of the impedance spectrum is typically a semicircle. The voltage ratio used to measure the current is known as an impedance system. It is measured through a range of frequencies and indirectly provides a spectrum of the reactions that occur [34].

The real (Z') and the imaginary (Z'') parts of the complex impedance of the Cole-Cole plot are expressed in the following equations:

$$Z' = Z_{\infty} + (Z_s - Z_{\infty}) \frac{1 + (\omega\tau)^n \cos(n\pi/2)}{1 + 2(\omega\tau)^n \cos(n\pi/2) + (\omega\tau)^{2n}} \quad (1)$$

$$Z'' = (Z_s - Z_{\infty}) \frac{(\omega\tau)^n \sin(n\pi/2)}{1 + 2(\omega\tau)^n \cos(n\pi/2) + (\omega\tau)^{2n}} \quad (2)$$

Where Z_s : Static impedance
 Z_{∞} : Impedance at a higher frequency
 τ : Relaxation time ($1/\omega$)
 ω : Angular frequency ($2\pi f$)
 n : Debye relaxation type ($0 \leq n \leq 1$)

A graph plotted with the imaginary part against the real part is known as a Cole-Cole plot. Based on Figure 12, the intersection of the semi-circular curve with the X-axis gives the bulk resistance (R_b) value of the HRP/PT/PPY/PANI film. The graph shows that the value of R_b increased (R_{b1} : 8.0Ω and R_{b2} : 14.0Ω), due to the polarity effect as the accumulated charge was reduced, leading to a reduction in the conductivity of the material. When a dielectric is placed in an electric field, the electrical charge does not flow through the conductive material, but only shifts slightly from its equilibrium position, causing electrical polarization [33].

CONCLUSION

HRP immobilization was performed on PANI, PPY and PT to investigate the effect of immobilization on HRP/PANI, HRP/PPY and HRP/PT without combining the three polymers simultaneously. The optical absorption spectra and bond formation, as characterized by UV-Vis and FTIR, indicated the relationship between the two materials. The conductivity areas represented by bright colours proved the conductivity of the PANI, PPY and PT surfaces, and

that HRP stabilization on the PT/PPY/PANI surfaces did not affect their conductivity. This finding was further confirmed by the resistance values obtained through the Four-Point Probe analysis. Further immobilization of HRP on the surface of PT/PPY/PANI provided a clearer picture of the suitability of the polymer as a polymeric support for enzyme activity. In addition, this study found that the surface roughness increased when HRP was immobilized onto the polymer layers, due to the small size of HRP that allowed the molecule to penetrate the polymer layers. On the other hand, this study also demonstrated the bond formation between PT/PPY/PANI and HRP as evidenced by their FTIR spectra. Furthermore, at a temperature of 4°C the resistance value was found to be lower compared to that at 27°C and 60°C after 25 days of evaluation, demonstrating the stability of HRP and its suitability for application under cold conditions. This finding was supported by its impedance values.

ACKNOWLEDGEMENTS

The authors would like to thank the Faculty of Applied Sciences and Technology, Universiti Tun Hussein Onn Malaysia and Faculty of Science and Technology, Universiti Kebangsaan Malaysia for the facilities provided.

REFERENCES

1. Ram, M. K. and Malhotra, B. D. (1996) Preparation and characterization of Langmuir-Blodgett films of polymeraldine base. *Journal of Polymer*, **37**, 4809–4813.
2. Watanabe, I., Hong, K. and Rubner, M. F. (1990) Langmuir-Blodgett manipulation of poly (3-alkylthiophenes). *Journal of Langmuir*, **6**, 1164–1172.

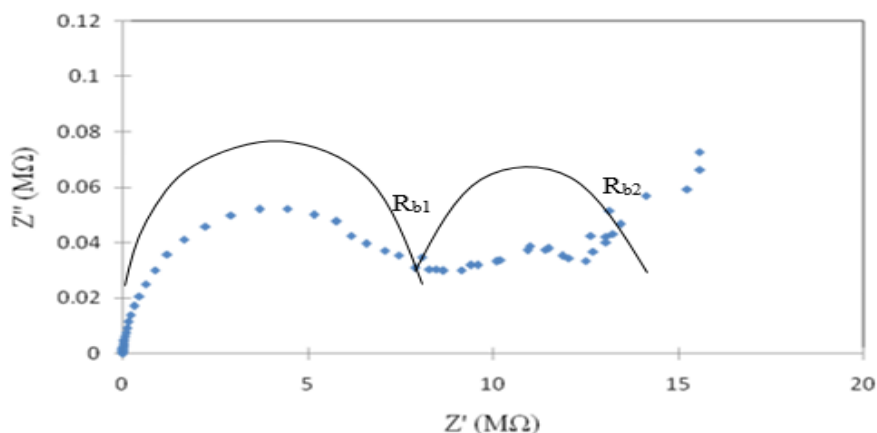


Figure 12. Cole-Cole plot of complex impedance for HRP/PT/PPY/PANI film at $T = 4^\circ\text{C}$

3. Shimazaki, Y., Mitsuishi, M., Ito, S. and Yamamoto, M. (1997) Preparation of the layer-by-layer deposited ultrathin film based on the charge-transfer interaction. *Journal of Langmuir*, **13**, 1385.
4. Skotheim, T. A. (Ed). (1986) *Handbook of conducting polymers, Vol 2*. New York: Marcel Dekker Inc.
5. Saxena, V. and Malhotra, B. D. (2003) Prospects of conducting polymers in molecular electronics. *Journal of Current applied physics*, **3**, 293–305.
6. Riu, I. Jr., A., Mattoso, L. H. C., Mattoso, S. V., Telles, G. D. and Oliveira Jr, O. N. (1995) Langmuir and Langmuir Blodgett films of parent polyaniline doped with functionalized acids. *Journal of Synthetic Metals*, **71**, 2067–2068.
7. Anderson, J. H. and Parks, G. A. (1968) The electrical conductivity of silica gel in the presence of adsorbed water. *Journal of Physical Chemistry*, **72**, 3662–3668.
8. Traversa, E. (1995) Ceramic sensors for humidity detection: the state-of-the-art and future developments. *Journal of Sensors and Actuators B*, **23**, 135–156.
9. Fubini, B., Bolis, V., Bailes, M. and Stone, F. S. (1989) The reactivity of oxides with water vapour. *Journal of Solid State Ionics*, **32-33**, 258–272.
10. Welinder, K. G., Gajhede, M., Anette, H., Jens, F. W. P., Anders, S. and Jorn, H. (1992) Crystallization and preliminary X-ray diffraction studies of a peroxidase from barley grain. *Journal of Molecular Biology*, **228**, 690–692.
11. Mohsina Hamid and Khalil-ur-Rehman. (2009) Potential applications of peroxidases. *Journal of Food Chemistry*, **115**, 1177–1186.
12. Pauliukaite, R., Chiorcea Paquim, A. M., Oliveira Brett, A. M. and Brett, M. A. (2006) Electrochemical, EIS and AFM characterisation of biosensors: Trioxysilane sol-gel encapsulated glucose oxidase with two different redox mediators. *Journal of Electrochemica Acta*, **52**, 1–8.
13. Zheng, Y. L., Huang, Y. F., Jiang, J. H., Zhang, X. B., Tang, C. R., Shen, G. L. and Yu, R. Q. (2007) Functionalization of multi-walled carbon nanotubes with poly (amidoamine) dendrimer for mediator-free glucose biosensor. *Journal of Electrochemistry Communications*, **9**, 185–190.
14. Kumaran Ramanathan, Ram, M. K., Malhotra, B. D. and Surya N. Murthy, A. (1995) Application of polyaniline Langmuir-Blodgett films as a glucose biosensor. *Journal of Materials Sciences and Engineering C*, **3**, 159–163.
15. Moralesa, A., Ckspedes, F., Mufiozb, J., Martinez-Fbregasa, E. and Alegret, S. (1996) Hydrogen peroxide amperometric biosensor based on a peroxidase-graphite-epoxy biocomposite. *Journal of Analytica Chimica Acta*, **332**, 131–138.
16. Singh H. N. (1997) *Handbook of Organic Conductive Molecules and Polymers, Vol 2*. River Street: John Wiley & Sons Ltd.
17. Douglas, A. S. and Donald, M. W. (1971) *Principles of Instrumental Analysis*, Austin: Holt, Rinehart and Winston Inc.
18. Sambhu Bhadra, Dipak Khastgir, Nikhil K. Singha and Joong Hee Lee (2009) Progress in preparation, processing and applications of polyaniline. *Journal of Progress polymer Science*, **34**, 783–810.
19. Singh, H. N. (1997b) *Handbook of Organic Conductive Molecules and Polymers, Vol 1*. River Street: John Wiley & Sons Ltd.
20. Peng Wang, Shengqi Li and Jinqing Kan (2009) A Hydrogen peroxide biosensor based on polyaniline/FTO. *Journal of Sensors and Actuators B*, **137**, 662–668.
21. Nigel C. Veitch (2004) Horseradish peroxidase: a modern view of a classic enzyme. *Journal of Phytochemistry*, **65**: 249–259.
22. Goel, S., Gupta, A., Singh, K. P., Mehrotra, R. and Kandpal, H. C. (2007) Optical studies of polyaniline nanostructures. *Journal of Materials Sciences and Engineering A*, **443**, 71–76.
23. Kevin, D. O., Heming, H., Peter, K., David, W. S. and Oleg, A. S. (2008) Anisotropy of local electrical conductivity of hyper-stoichiometric uranium dioxide revealed by current-sensing atomic force microscopy (CS-AFM). *Journal of Electrochemistry Communications*, **10**, 1805–1808.
24. Fabio, L. L., Mario de Oliveira, N., Leonardo, G. P., Michel, R. M. B., Igor, P., Yvonne, P. M., Paulo, S. P. H., Luiz, H. C. M. and Osvaldo, N. O. Jr. (2007) Nanoscale conformational ordering in polyanilines investigated by SAXS and AFM.

- Journal of Colloid and Interface Science*, **316**, 376–387.
25. Omaish, M. A. and Faiz, M. (2011) Thermal stability, electrical conductivity and ammonia sensing studies on *p*-toluenesulfonic acid doped polyaniline: titanium dioxide (pTsa/Pani: TiO₂) nanocomposites. *Journal of Sensors and Actuators B: Chemical*, **157**, 122–129.
 26. Havriliak, S. and Negami, S. (1967) A complex plane representation of dielectric and mechanical relaxation process in some polymers. *Journal of Polymer*, **8**, 161–210.
 27. Singh, H. N. (1997) *Handbook of Organic Conductive Molecules and Polymers, Vol 1*. River Street: John Wiley & Sons Ltd.
 28. Kafi, A. K. M., Dong-Yun, L., Won-Suk, C. and Young-Soo, K. (2008) Fabrication and electrochemical characterization of HRP-lipid Langmuir-Blodgett film and its application as an H₂O₂ biosensor. *Journal of Thin Solid Films*, **516**, 3641–3645.
 29. Fernandes, K. F., Lima, C. S., Lopes, F. M. and Collins, C. H. (2004) Properties of Horseradish peroxidase immobilised onto polyaniline. *Journal of Process Biochemistry*, **39**, 957–962.
 30. Zhang, X., Goux, W. J. and Manohar, S. K. (2004) Synthesis of Polyaniline Nanofibers by “Nanofiber Seeding”. *Journal of American Chemical Society*, **126**, 4502–4503.
 31. Chen, C. W., Hua, J. and Liu, T. J. (2007) Stable Langmuir-Blodgett film deposition of polyaniline and arachidic acid. *Journal of Thin Solid Films*, **515**, 7299–7306.
 32. Sabapathy Manigandan, Anudeep Jain, Saptarshi Majumder, Saibal Ganguly and Kajari Kagupta (2008) Formation of nanorods and nanoparticles of polyaniline using Langmuir- Blodgett technique: Performance study for ammonia sensor. *Journal of Sensors and Actuators B*, **133**, 182–194.
 33. Raja, V.K., Sharma, A. K. and Narasimha Rao, V. V. R. (2004) Impedance spectroscopic and dielectric analysis of PMMA-CO-P4VPNO polymer films. *Journal of Materials Letters*, **58**, 3242–3247.
 34. Cesar, F. S., Calum, J. M. and Keith R. (2005) Electrochemical impedance spectroscopy studies of polymer degradation: application to biosensor development. *Trends in Analytical Chemistry*, **24**, 1.
 35. Li, M, Wu, J, Su, H, T,u Y, Shang, Y, He, Y and Liu, H. (2019) Ionic Liquid-Polypyrrole-Gold Composites as Enhanced Enzyme Immobilization Platforms for Hydrogen Peroxide Sensing. *Sensors (Basel)*, **19**, 640.
 36. Namsheer, K. and Chandra Sekhar Rout (2021) Conducting polymers: a comprehensive review on recent advances in synthesis, properties and applications. *RSC Advances*, **11**, 5659–5697.
 37. Rahaman, M, Aldalbahi, A, Almoiqli, M, Alzahly, S. (2018) Chemical and Electrochemical Synthesis of Polypyrrole Using Carrageenan as a Dopant: Polypyrrole/Multi-Walled Carbon Nanotube Nano-composites. *Polymers (Basel)*, **10**, 632.
 38. Bhalla, N, Jolly, P, Formisano, N, Estrela, P. (2016) Introduction to biosensors. *Essays Biochem.* **60**, 1–8.
 39. Han Ju Lee, Andrew C. Jamison and T. Randall Lee. (2015) Surface Dipoles: A Growing Body of Evidence Supports Their Impact and Importance. *Accounts of Chemical Research*, **48**, 3007–3015.
 40. Song Ye, Lv Huiling, Hu Songwei, Yang Chunyan and Zhu Xufei. (2013) Electroactivity of Polyaniline in High pH Solutions. *Acta Chimica Sinica- Chinese Edition*, **71**, 999.
 41. Fei Shen, Simin Arshi, Edmond Magner, Jens Ulstrup and Xinxin Xiao (2022) One-step electrochemical approach of enzyme immobilization for bioelectrochemical applications. *Synthetic Metals*, **291**, 117205.